Available online at www.sciencedirect.com
ScienceDirect
ELSEVIER
J. Differential Equations 233 (2007) 181–198
Journal of Differential Equations
www.elsevier.com/locate/jde

Interval analysis techniques for boundary value problems of elasticity in two dimensions

Irina Mitrea [a,1], Warwick Tucker [b,*,2]

[a] *Department of Mathematics, University of Virginia, Kerchof Hall, Charlottesville, VA 22904, USA*
[b] *Department of Mathematics, Uppsala University, Box 480, Uppsala, Sweden*

Received 3 March 2006

Available online 17 November 2006

Abstract

In this paper we prove that the L^2 spectral radius of the *traction* double layer potential operator associated with the Lamé system on an infinite sector in $\mathbb{R}^2$ is within 10^{-2} from a certain conjectured value which depends explicitly on the aperture of the sector and the Lamé moduli of the system. This type of result is relevant to the spectral radius conjecture, cf., e.g., Problem 3.2.12 in [C.E. Kenig, Harmonic Analysis Techniques for Second Order Elliptic Boundary Value Problems, CBMS Reg. Conf. Ser. Math., vol. 83, Amer. Math. Soc., Providence, RI, 1994]. The techniques employed in the paper are a blend of classical tools such as Mellin transforms, and Calderón–Zygmund theory, as well as interval analysis—resulting in a computer-aided proof.

MSC: primary: 45E05, 47A05; secondary: 35J25, 42B20

Keywords: Lamé system; Layer potentials; Traction conormal derivative; Spectral radius; Interval analysis; Computer-aided proof

1. Introduction

The iterative approach for solving boundary value problems of mathematical physics which lead to an equation of the form $x - Lx = g$ is the method of successive approximations based on

* Corresponding author.
E-mail addresses: im3p@virginia.edu (I. Mitrea), warwick@math.uu.se (W. Tucker).
1 Supported in part by the NSF Grant DMS 0547944 and a University of Virginia FEST Grant.
2 Research fellow of the Royal Swedish Academy of Sciences.

0022-0396/$ – see front matter
doi:10.1016/j.jde.2006.10.010

the scheme

$$x^{k+1} = L\left(x^k\right) + g. \tag{1.1}$$

Here L is a bounded linear operator on a Banach space $\mathcal{X}$ and $g \in \mathcal{X}$ is given. The size of $\rho(L; \mathcal{X})$, *the spectral radius of L on $\mathcal{X}$*, is important in establishing the convergence of (1.1). For instance, when

$$\rho(L; \mathcal{X}) < 1, \tag{1.2}$$

and $x_0 = 0$, the iteration (1.1) converges to a solution of $x - Lx = g$ as the Neumann series $\sum_{k=0}^{\infty} L^k$ converges to $(I - L)^{-1}$ in the operator norm (I is the identity on $\mathcal{X}$).

An important question at the interface between harmonic analysis and partial differential equations is the so-called spectral radius conjecture for elliptic boundary layers on rough domains, which is singled out as a challenging open problem in Kenig's 1994 AMS CBMS book [10]. This problem asks whether (1.2) holds whenever L is a double layer potential operators associated with the Laplacian (or Lamé and Stokes systems) and $\mathcal{X} = L^p(\partial\Omega)$, for a Lipschitz domain Ω, whenever $I - L$ is invertible. This issue is relevant in the context of constructively solving boundary value problems arising in the study of the Stokes flow and elastic deformations.

In this paper we consider the case when L is a singular integral operator naturally associated with the traction boundary value problem for the system of elastostatics in an infinite sector $\Omega \subseteq \mathbb{R}^2$,

$$\begin{cases} \mu\Delta\vec{u} + (\lambda + \mu)\nabla \operatorname{div} \vec{u} = \vec{0} & \text{in } \Omega, \\ \frac{\partial \vec{u}}{\partial N_\mu} = \vec{f} \in L^2(\partial\Omega), \end{cases} \tag{1.3}$$

where the Lamé moduli μ, λ satisfy $\mu > 0$ and $\lambda + \mu \geqslant 0$, and $\frac{\partial}{\partial N_\mu}$ denotes the traction conormal derivative (2.3). More specifically, we take L in (1.1) to be K^*, the formal adjoint of the so-called traction double layer potential operator K (introduced in Section 2.) We would like to point out that the case under consideration is both physically relevant and, from a technical standpoint, the most challenging among all Neumann-type boundary problems for the system of elastostatics. Indeed, the spectral analysis of K undertaken here is considerably more difficult and subtle than the one for the layer potential operator associated with the *pseudo-stress* conormal derivative, considered previously in [17,18].

For $\alpha \in [0, \pi]$, $\kappa \in [0, 1]$ and $x \in (0, 1)$ we introduce

$$\begin{aligned} R(\alpha, x, \kappa) := \Big| &\big\{\sin^2(\alpha x) + \kappa^2 \cos^2(\alpha x) - \big(\kappa \cos(\pi x) - (1 - \kappa) x \sin\alpha \sin(\alpha x)\big)^2\big\}^{1/2} \\ &+ (1 - \kappa) x \sin\alpha \cos(\alpha x)\Big| \cdot \frac{1}{\sin(\pi x)}. \end{aligned} \tag{1.4}$$

Our main result gives estimates for $\rho(K; L^2(\partial\Omega))$ (which equals $\rho(K^*; L^2(\partial\Omega))$) for a family of infinite sectors in $\Omega \subset \mathbb{R}^2$ which pin $\rho(K; L^2(\partial\Omega))$ within 10^{-2} from a certain conjectured value which depends explicitly on μ, λ and the aperture of Ω. Concretely we have

Theorem 1.1. *Let $\Omega \subset \mathbb{R}^2$ be an infinite sector of aperture $\theta \in (0, 2\pi)$ and let K be the traction double layer potential operator associated with* (1.3) *and set $\kappa := \mu/(2\mu + \lambda) \in [\frac{1}{40}, \frac{9}{10}]$. Then, for $\theta \in [\frac{\pi}{200}, 2\pi - \frac{\pi}{200}]$, we have*

$$R\big(|\pi - \theta|, 1/2, \kappa\big) \leqslant \rho\big(K; L^2(\partial\Omega)\big) \leqslant R\big(|\pi - \theta|, 1/2, \kappa\big) + 10^{-2}. \tag{1.5}$$

In fact, prior experiments with the problem led the present authors to conjecture the following.

Conjecture. *If $\Omega \subseteq \mathbb{R}^2$ is an infinite sector of aperture $\theta \in (0, 2\pi)$ and $1 < p < \infty$, then*

$$\rho\big(K; L^p(\partial\Omega)\big) = R\big(|\pi - \theta|, 1/p, \kappa\big), \tag{1.6}$$

where $\kappa := \mu/(2\mu + \lambda) \in (0, 1]$.

Traditionally, the major theoretical tools involved in the study of the spectra of singular integral operators are Calderón–Zygmund theory (for layer potential operators on Lipschitz domains; see, e.g., the work of Fabes, Kenig, Verchota and Escauriaza in [4,6,28]) and Mellin transform techniques (for layer potentials on domains with isolated singularities; see, e.g., the work of Elschner, Fabes, Lewis, Maz'ya and collaborators and Shelepov in [5,7,8,11,12,15,16,24]). The main novel aspect of our present work is the realization that the use of *interval analysis* and rigorous computations (employed by Tucker in [26,27] to prove Smale's 14th problem concerning the existence of the Lorenz attractor) can play a significant role in the study of spectral problems of the type described above. Indeed, the proof of our main result combines Mellin transform and interval analysis techniques.

The strategy for obtaining lower bounds for $\rho(K; L^2(\partial\Omega))$ consists of the following steps. First, the spectrum of the operator K on $L^2(\partial\Omega)$ can be expressed as an (explicit) parametric curve in the plane, depending on the aperture of the sector θ and on $\kappa := \mu/(2\mu + \lambda)$,

$$[-\infty, \infty] \ni y \mapsto \Sigma_{\theta,\kappa}(y) \in \mathbb{R}^2. \tag{1.7}$$

This is possible in the current geometrical context as the operator K is of Mellin convolution type when $\Omega \subset \mathbb{R}^2$ is an infinite sector. Second, one writes

$$\rho\big(K; L^2(\partial\Omega)\big) = \sup_{-\infty \leqslant y \leqslant \infty} \big|\Sigma_{\theta,\kappa}(y)\big| \geqslant \big|\Sigma_{\theta,\kappa}(0)\big|, \tag{1.8}$$

and the last expression can be seen to match the left-hand sides in (1.5).

As for the upper bound for $\rho(K; L^2(\partial\Omega))$ we show that for every $y \in [-\infty, \infty]$, $\kappa \in [\frac{1}{40}, \frac{9}{10}]$, and $\theta \in [\frac{\pi}{200}, 2\pi - \frac{\pi}{200}]$, we have

$$\big|\Sigma_{\theta,\kappa}(y)\big| < R\big(|\theta - \pi|, 1/2, \kappa\big) + 10^{-2}. \tag{1.9}$$

Somewhat more specifically, a rough analytic approach is taken for checking (1.9) for $|y| > 10^4$. For the remaining part, i.e., $y \in [-10^4, 10^4]$, we use interval analysis techniques to rigorously carry out—using the computer—this latter (more delicate) task. Interval analysis is based on the idea that all computations using the computer should be carried out over sets rather than single points in the traditional manner. As the name suggests, these sets are (closed) intervals of the real line, or boxes in higher dimensions. The main advantages of this approach are that all *rounding errors* can easily (and automatically) be taken into account by switching the computer's internal rounding mode at run-time; and that all *discretization errors* can be taken into account since all entities are set-valued.

In the present case, both the parametric curve $|\Sigma_{\theta,\kappa}|$, and the function $R(\alpha, x, \kappa)$ will be made interval-valued, and 10^{-2} will be taken as the upper bound on all errors made when evaluating the distance between these two entities. The interval-based approach enables us then to check using the computer that (1.9) holds on the compact domain in the parameter space given by $\theta \in [\frac{\pi}{200}, 2\pi - \frac{\pi}{200}]$, $\kappa \in [\frac{1}{40}, \frac{9}{10}]$, $y \in [-10^4, 10^4]$. We stress that, even though the proof is computer-aided, it is rigorous in the mathematical sense. For a concise reference on the mathematics behind interval analysis, see, e.g., [1,13,20,21], or [22].

The analytical part of the proof of the main result is carried out for all $1 < p < \infty$ and allows for 10^{-6} instead of 10^{-2} in (1.9). For the computational part of the proof, however, a better accuracy and allowing for an interval of $p's$ instead of a single value increases tremendously (at least by a factor of 10^3) the running time of the algorithms involved. As is, the computer-aided part of the proof requires 16 hours of running time on 5 parallel processes. Nevertheless, the spectral radius estimates (1.5) are, from the point of view of a large number of engineering applications, as effective as (1.6).

The layout of the paper is as follows. Section 2 contains some preliminary notations and definitions as well as known results. In Section 3 we take the first (analytical) step toward proving the main result while in Section 4 we present the validated numerics part of the proof. Finally, in Section 5, a connection with the spectral radius conjecture is made.

2. Preliminaries

In this section we introduce some basic notation and recall some known results used in the rest of the paper. Hereafter Ω will be an infinite sector of aperture $\theta \in (0, 2\pi)$, i.e., the domain in $\mathbb{R}^2$ consisting of the interior of an infinite angle of measure θ. We let $d\sigma$ stand for the arc-length measure on $\partial\Omega$. Then the unit normal vector $N = (N_1, N_2)$ to $\partial\Omega$ is well defined at almost every point on $\partial\Omega$ with respect to $d\sigma$. We also use $\langle\cdot,\cdot\rangle$ to denote the canonical inner product in $\mathbb{R}^2$.

Consider next the system of elastostatics

$$\mathcal{L}\vec{u} = \mu\Delta\vec{u} + (\lambda + \mu)\nabla \operatorname{div} \vec{u} = 0 \quad \text{in } \Omega, \tag{2.1}$$

where the so-called Lamé moduli μ, λ satisfy

$$\mu > 0 \quad \text{and} \quad \lambda + \mu \geqslant 0. \tag{2.2}$$

The *traction* (*stress*) conormal derivative of a vector $\vec{u}$ (cf., e.g., [4]) has the form

$$\frac{\partial\vec{u}}{\partial N_\mu} := \mu\big(\nabla\vec{u} + (\nabla\vec{u})^t\big)N + \lambda(\operatorname{div}\vec{u})N, \tag{2.3}$$

where $\nabla\vec{u} = (\partial_j u^i)_{1\leqslant i,j\leqslant 2}$, and the superscript t indicates transposition of matrices. Recall next the Kelvin matrix valued fundamental solution for the system of elastostatics (2.1) given at each $X = (X_1, X_2) \in \mathbb{R}^2 \setminus \{0\}$ by

$$G_{ij}(X) = \frac{1}{2\mu(2\mu+\lambda)\pi}\left[\frac{3\mu+\lambda}{2}\delta_{ij}\log|X|^2 - (\mu+\lambda)\frac{X_iX_j}{|X|^2}\right], \quad i,j=1,2. \tag{2.4}$$

See, e.g., (9.2) in Chapter 9 of [14]. In (2.4), δ_{ij} denotes the Kronecker symbol. For $j = 1, 2$, let G^j be the jth column of the matrix $G = (G_{kl})_{k,l=1,2}$. A straightforward computation gives that the ith component of $\frac{\partial G^j}{\partial N_\mu}$ is

$$\left(\frac{\partial G^j}{\partial N_\mu}(X-\cdot)\right)^i(Q) = -\frac{\kappa\delta_{ij}}{\pi}\cdot\frac{\langle X-Q, N(Q)\rangle}{|X-Q|^2} + \frac{\kappa}{\pi}\cdot\frac{(X_i-Q_i)N_j(Q)-(X_j-Q_j)N_i(Q)}{|X-Q|^2}$$
$$-\frac{2(1-\kappa)}{\pi}\cdot\frac{\langle X-Q, N(Q)\rangle(X_i-Q_i)(X_j-Q_j)}{|X-Q|^4} \tag{2.5}$$

where

$$\kappa := \frac{\mu}{2\mu+\lambda}. \tag{2.6}$$

We denote by K the traction double layer potential operator associated with the system (2.1) given by

$$(K\vec{f})(P) := \text{p.v.}\int_{\partial\Omega}\left[\frac{\partial G}{\partial N_\mu}(P-\cdot)\right]^t(Q)\vec{f}(Q)\,d\sigma(Q), \quad P\in\partial\Omega. \tag{2.7}$$

For $1 < p < \infty$, we denote by $L^p(\partial\Omega)$ the space of p-integrable functions on $\partial\Omega$. In the sequel we make no notational distinction between $L^p(\partial\Omega)$ and $L^p(\partial\Omega)\oplus L^p(\partial\Omega)$. Next, let $\mathcal{X}$ be a Banach space and $T:\mathcal{X}\to\mathcal{X}$ be a linear and continuous operator. We denote by $\sigma(T;\mathcal{X})$ the spectrum of the operator T given by

$$\sigma(T;\mathcal{X}) := \{z\in\mathbb{C}\colon\ zI-T \text{ is not invertible on } \mathcal{X}\}, \tag{2.8}$$

and by $\rho(T;\mathcal{X})$ the spectral radius of T, i.e.,

$$\rho(T;\mathcal{X}) := \sup\bigl\{|z|\colon\ z\in\sigma(T;\mathcal{X})\bigr\}. \tag{2.9}$$

With the goal of explicitly describing the spectrum of the operator K as in (2.7) on $L^p(\partial\Omega)$, $1 < p < \infty$, we introduce

$$A_\kappa := (1-\kappa)z\sin\theta, \qquad B := \sin\bigl((\pi-\theta)z\bigr), \qquad C := \cos\bigl((\pi-\theta)z\bigr),$$
$$D := \sin(\pi z), \qquad E := \cos(\pi z), \tag{2.10}$$

where $\theta,\kappa\in\mathbb{R}$ and $z\in\mathbb{C}$. Next we record the following result established in [19] by employing the pseudo-differential calculus of Mellin type.

Theorem 2.1. *Let $\Omega \subset \mathbb{R}^2$ be an infinite sector of aperture $\theta \in (0, 2\pi)$ and let K be the traction double layer potential operator associated with the system* (2.1) *with Lamé moduli λ, μ satisfying* (2.2)*. Then, for every $1 < p < \infty$, we have*

$$\sigma\bigl(K; L^p(\partial\Omega)\bigr) = \left\{w \in \mathbb{C}\colon (wD \pm A_\kappa C)^2 = Q_{\kappa,\mp} \text{ for some } z \in \frac{1}{p} + i\mathbb{R}\right\} \cup \{\kappa, -\kappa\}, \quad (2.11)$$

where κ is as in (2.6) *and A_κ, B, C, D* (*evaluated at z*) *are as in* (2.10)*. Also*

$$Q_{\kappa,\pm} := B^2 + \kappa^2 C^2 - (\kappa E \pm A_\kappa B)^2. \quad (2.12)$$

In particular

$$\sigma\bigl(K; L^p(\partial\Omega)\bigr) = \bigcup_{i=1}^{4} \Sigma_i(\theta, p, \kappa). \quad (2.13)$$

Above $[-\infty, \infty] \ni y \mapsto \Sigma_i(\theta, p, \kappa)(y) \in \mathbb{R}^2$ is a parametric closed curve in the plane, given by

$$\Sigma_1(\theta, p, \kappa)(y) := \frac{\sqrt{Q_{\kappa,-}} - A_\kappa C}{D}, \qquad \Sigma_2(\theta, p, \kappa)(y) := \frac{-\sqrt{Q_{\kappa,-}} - A_\kappa C}{D},$$
$$\Sigma_3(\theta, p, \kappa)(y) := \frac{\sqrt{Q_{\kappa,+}} + A_\kappa C}{D}, \qquad \Sigma_4(\theta, p, \kappa)(y) := \frac{-\sqrt{Q_{\kappa,+}} + A_\kappa C}{D}, \quad (2.14)$$

where A_κ, B, C, D, E are evaluated at $z = \frac{1}{p} + iy$, $y \in \mathbb{R}$.

We end this section with the simple, yet useful observation that for any $1 < p < \infty$, $y \in \mathbb{R}$ and $\theta \in \mathbb{R}$, we have

$$\Sigma_1(2\pi - \theta, p, \kappa)(y) = -\Sigma_2(\theta, p, \kappa)(y) \quad \text{and} \quad \Sigma_3(2\pi - \theta, p, \kappa)(y) = -\Sigma_4(\theta, p, \kappa)(y), \quad (2.15)$$

and

$$\Sigma_j(\theta, p, \kappa)(-y) = \overline{\Sigma_j(\theta, p, \kappa)(y)}, \quad \text{for } j = 1, \dots, 4, \quad (2.16)$$

where, if $z \in \mathbb{C}$, $\bar{z}$ denotes the complex conjugate of z.

3. Spectral radius estimates

Let Ω be an infinite sector in $\mathbb{R}^2$ and assume that $\mu > 0$, $\mu + \lambda \geqslant 0$. Next we recall the traction double layer potential operator K from (2.7) associated with the Lamé system (2.1) in Ω. Finally, for $\alpha \in [0, \pi]$, $x \in (0, 1)$ and $\kappa \in [0, 1]$ introduce

$$R(\alpha, x, \kappa) := \Bigl|\bigl\{\sin^2(\alpha x) + \kappa^2\cos^2(\alpha x) - \bigl(\kappa\cos(\pi x) - (1-\kappa)x\sin\alpha\sin(\alpha x)\bigr)^2\bigr\}^{1/2}$$
$$+ (1-\kappa)x\sin\alpha\cos(\alpha x)\Bigr| \cdot \frac{1}{\sin(\pi x)}. \quad (3.1)$$

Our main result here is

Theorem 3.1. *Let $\Omega \subseteq \mathbb{R}^2$ be an infinite sector of aperture $\theta \in (0, 2\pi)$. Consider μ, λ as in* (2.2) *such that $\frac{\mu}{2\mu+\lambda} \in [\frac{1}{40}, \frac{9}{10}]$ and let K be as in* (2.7)*. Then, for any $\theta \in [\frac{\pi}{200}, 2\pi - \frac{\pi}{200}]$ we have*

$$R\left(|\pi - \theta|, \frac{1}{2}, \frac{\mu}{2\mu+\lambda}\right) \leqslant \rho\big(K; L^2(\partial\Omega)\big) < R\left(|\pi - \theta|, \frac{1}{2}, \frac{\mu}{2\mu+\lambda}\right) + 10^{-2}. \tag{3.2}$$

Before presenting the proof of Theorem 3.1 we isolate first the main analytical ingredients. As a preamble, we start with the following technical result.

Lemma 3.2. *For any $\alpha \in [0, \pi]$, $\kappa \in [0, 1]$ and $x \in (0, \frac{1}{2}]$ we have*

$$R(\alpha, x, \kappa) \geqslant \kappa. \tag{3.3}$$

Proof. Straightforward algebraic manipulations based on (3.1) show that for (3.3) the following inequality suffices

$$E(\alpha, x, \kappa) \geqslant \big(\kappa \sin(\pi x) - x(1-\kappa)\sin(\alpha)\cos(\alpha x)\big)^2, \quad \forall \alpha \in [0, \pi],\ x \in \left(0, \frac{1}{2}\right],\ \kappa \in [0, 1], \tag{3.4}$$

where

$$E(\alpha, x, \kappa) := \sin^2(\alpha x) + \kappa^2 \cos^2(\alpha x) - \big(\kappa \cos(\pi x) - x(1-\kappa)\sin(\alpha)\cos(\alpha x)\big)^2. \tag{3.5}$$

Expanding the square and using the Pythagorean identity we rewrite the latter inequality in the equivalent form

$$(1-\kappa) f(\alpha, x, \kappa) \geqslant 0, \tag{3.6}$$

where

$$f(\alpha, x, \kappa) := (1+\kappa)\sin^2(\alpha x) - x^2(1-\kappa)\sin^2(\alpha) + 2x\kappa \sin(\alpha)\sin\big((\pi+\alpha)x\big), \tag{3.7}$$

for α, x and κ as in (3.4). Notice next that the partial derivative with respect to κ of $f(\alpha, x, \kappa)$ equals $\sin^2(\alpha x) + x^2 \sin^2(\alpha) + 2x \sin(\alpha)\sin((\pi+\alpha)x)$ which is positive whenever $\alpha \in [0, \pi]$ and $x \in [0, \frac{1}{2}]$. Therefore for α and x as above and $\kappa \geqslant 0$ we have

$$f(\alpha, x, \kappa) \geqslant f(\alpha, x, 0) = \sin^2(\alpha x) - x^2 \sin^2(\alpha) \geqslant 0, \tag{3.8}$$

where the inequality in (3.8) follows from squaring (5.2) and the observation that $\sin(\alpha x)$ and $x\sin(\alpha)$ are positive for α and x as in (3.4). Finally, (3.6) immediately follows from (3.8). □

Proposition 3.3. *Let $\theta \in [0, \pi]$, $x \in (0, 1]$, $\kappa \in [0, 1]$, $|y| \in [1, \infty)$ and recall A_κ, B, C, D, E from* (2.10). *Then the following hold*

$$\max\left\{\frac{|C|}{|D|}, \frac{|B|}{|D|}, \frac{|A_\kappa B|}{|D|}, \frac{|A_\kappa C|}{|D|}, 2\kappa\frac{|EA_\kappa B|}{|D^2|}, \frac{\kappa}{|D|}\right\} \leqslant 50|y|e^{-\theta|y|}. \tag{3.9}$$

In particular, if $\theta \in [\frac{\pi}{200}, \pi]$ and $|y| \geqslant 10^4$, we have

$$\max\left\{\frac{|C|}{|D|}, \frac{|B|}{|D|}, \frac{|A_\kappa B|}{|D|}, \frac{|A_\kappa C|}{|D|}, 2\kappa\frac{|EA_\kappa B|}{|D^2|}, \frac{\kappa}{|D|}\right\} \leqslant 10^{-14}. \tag{3.10}$$

Proof. Fix $\theta \in [0, \pi]$, $x \in (0, 1]$, $\kappa \in [0, 1]$ and $|y| \in [1, \infty)$. Then, based on (2.10) we have

$$|A_\kappa| = \left|(1-\kappa)(x+iy)\sin(\theta)\right| \leqslant |x+iy| \leqslant \sqrt{2}|y|. \tag{3.11}$$

Also

$$\begin{aligned} 4|D|^2 &= e^{2\pi y} + e^{-2\pi y} - 2\cos(2\pi x) \geqslant \left(e^{\pi y} - e^{-\pi y}\right)^2, \\ 4|E|^2 &= e^{2\pi y} + e^{-2\pi y} + 2\cos(2\pi x) \leqslant \left(e^{\pi y} + e^{-\pi y}\right)^2. \end{aligned} \tag{3.12}$$

Therefore

$$|D| \geqslant \frac{e^{\pi|y|} - e^{-\pi|y|}}{2} \geqslant \frac{1}{4}e^{\pi|y|} \quad \text{and} \quad |E| \leqslant \frac{e^{\pi|y|} + e^{-\pi|y|}}{2} \leqslant e^{\pi|y|}. \tag{3.13}$$

Going further, $4|B|^2 = e^{2\alpha y} + e^{-2\alpha y} - 2\cos(2\alpha x) \leqslant (e^{\alpha y} + e^{-\alpha y})^2$, where $\alpha := \pi - \theta$. This, and a similar analysis for $|C|$ give

$$\max\{|B|, |C|\} \leqslant \frac{e^{\alpha|y|} + e^{-\alpha|y|}}{2} \leqslant e^{\alpha|y|}. \tag{3.14}$$

Now, (3.9) follows from (3.11), (3.13) and (3.14) and straightforward algebraic manipulations. Next fix $\theta \in [\frac{\pi}{200}, \pi]$ and consider $F : [0, \infty) \to \mathbb{R}$ given by $F(t) := te^{-\theta t}$. A simple analysis reveals that F is decreasing on the interval $[\frac{1}{\theta}, \infty)$. Since for $\theta \geqslant \frac{\pi}{200}$ and $|y| \geqslant 10^4$ we have $|y| \geqslant \frac{100}{\theta} > \frac{1}{\theta}$, using the monotonicity of F we conclude

$$|y|e^{-\theta|y|} = F\big(|y|\big) \leqslant F\left(\frac{100}{\theta}\right) = \frac{100}{\theta \cdot e^{100}} \leqslant \frac{2 \times 10^4}{\pi \cdot e^{100}} \leqslant 10^{-16}. \tag{3.15}$$

Now, (3.10) follows from (3.9) and (3.15) and the proof of Proposition 3.3 is finished. □

Corollary 3.4. *Let μ, λ be as in* (2.2) *and recall the parametric curves $\Sigma_i(\theta, p, \kappa)$, $i = 1, \ldots, 4$, introduced in* (2.14) *where κ is as in* (2.6). *Then, for all $1 < p < \infty$, $\theta \in [\frac{\pi}{200}, 2\pi - \frac{\pi}{200}]$ and $|y| \geqslant 10^4$, we have*

$$\left|\Sigma_i(\theta, p, \kappa)(y)\right| < R\left(|\pi - \theta|, \frac{1}{p}, \kappa\right) + 10^{-6}. \tag{3.16}$$

Proof. In the light of (2.15) matters can be reduced, without loss of generality, to the case $\theta \in [\frac{\pi}{200}, \pi]$. In this scenario, fix μ, λ, and p as in the hypothesis and set $w(y) := \Sigma_1(\theta, p, \kappa)(y)$ where κ is as in (2.6). Using the triangle inequality in (2.14) it immediately follows that

$$\left|w(y)\right| \leqslant \frac{|\sqrt{Q_{\kappa,-}}\,|}{|D|} + \frac{|A_\kappa C|}{|D|}. \tag{3.17}$$

Next, using (2.10) and the fact that $D^2 + E^2 = 1$ we obtain

$$\left|\frac{Q_{\kappa,-} - \kappa^2 D^2}{D^2}\right| = \left|\frac{B^2 + \kappa^2 C^2 - 2\kappa E A_\kappa B - A_\kappa^2 B^2 - \kappa^2}{D^2}\right|. \tag{3.18}$$

Recall here that $\kappa := \frac{\mu}{2\mu+\lambda} \in [0, 1]$. Moreover, if $|y| \geqslant 10^4$, by (3.10) and the triangle inequality we have that the right-hand side in (3.18) does not exceed $4 \times 10^{-28} + 10^{-14}$. In particular,

$$\left|\frac{Q_{\kappa,-} - \kappa^2 D^2}{D^2}\right| < 10^{-13} \quad \text{and} \quad \left|\frac{\sqrt{Q_{\kappa,-}}}{D}\right| \leqslant \sqrt{10^{-13} + \kappa^2} < 2. \tag{3.19}$$

On the other hand, since $(w(y)D + A_\kappa C)^2 = Q_-$ we obtain

$$\left(w^2(y) - \kappa^2\right)D^2 = Q_{\kappa,-} - \kappa^2 D^2 - 2w(y)A_\kappa C D - A_\kappa^2 C^2. \tag{3.20}$$

Using the triangle inequality we further infer that

$$\left|w^2(y) - \kappa^2\right| \leqslant \frac{|Q_{\kappa,-} - \kappa^2 D^2|}{|D|^2} + 2\left|w(y)\right|\frac{|A_\kappa C|}{|D|} + \frac{|A_\kappa C|^2}{|D|^2}, \tag{3.21}$$

and therefore by (3.17), (3.19) and (3.10) we have

$$\left|w^2(y) - \kappa^2\right| < 10^{-13} + 2 \times 10^{-14}\left(2 + 10^{-14}\right) + 10^{-28} < 10^{-12}. \tag{3.22}$$

Finally from (3.22), employing again the triangle inequality, we have that $|w^2(y)| \leqslant \kappa^2 + 10^{-12} \leqslant (\kappa + 10^{-6})^2$. Taking square root in both sides of the previous inequality further gives

$$\left|w(y)\right| \leqslant \kappa + 10^{-6} < R\left(\pi - \theta, \frac{1}{p}, \kappa\right) + 10^{-6}, \tag{3.23}$$

where the last inequality is a consequence of (3.3) from Lemma 3.2. This gives (3.16) when $i = 1$ and the cases $i \in \{2, 3, 4\}$ follow in a similar manner. □

4. Validated numerics

In this section we describe how the computer-assisted part of the proof of Theorem 3.1 is structured. We start with a brief introduction of the underlying mathematics that enables the computer to rigorously verify that

$$\left|\Sigma_i(\theta, 2, \kappa)(y)\right| < R\left(|\pi - \theta|, \frac{1}{2}, \kappa\right) + 10^{-2}, \quad i = 1, \ldots, 4, \tag{4.1}$$

for all μ, λ as in (2.2) such that $\kappa := \frac{\mu}{2\mu+\lambda} \in [\frac{1}{40}, \frac{9}{10}]$, $y \in [-10^4, 10^4]$ and $\theta \in [\frac{\pi}{200}, 2\pi - \frac{\pi}{200}]$. This, in concert with (3.16) in Corollary 3.4, finishes the proof of Theorem 3.1.

4.1. Interval analysis

The foundation of most computer-aided proofs dealing with continuous problems is the ability to compute with set-valued functions. This not only allows for all rounding errors to be taken into account, but—more importantly—all discretization errors too. Here, we will briefly describe the fundamentals of interval analysis. For a concise reference on this topic, see, e.g. [1,13,20,21], or [22].

Let $\mathbb{IR}$ denote the set of closed intervals. For any element $\mathbb{A} \in \mathbb{IR}$, we adopt the notation $\mathbb{A} = [\underline{\mathbb{A}}, \overline{\mathbb{A}}]$, where $\underline{\mathbb{A}}, \overline{\mathbb{A}} \in \mathbb{R}$. If $\star$ is one of the operators $+, -, \times, \div$, we define the arithmetic on elements of $\mathbb{IR}$ by

$$\mathbb{A} \star \mathbb{B} = \{a \star b\colon\ a \in \mathbb{A},\ b \in \mathbb{B}\},$$

except that $\mathbb{A} \div \mathbb{B}$ is undefined if $0 \in \mathbb{B}$. Working exclusively with closed intervals, we can describe the resulting interval in terms of the endpoints of the operands:

$$\begin{aligned} \mathbb{A} + \mathbb{B} &= [\underline{\mathbb{A}} + \underline{\mathbb{B}}, \overline{\mathbb{A}} + \overline{\mathbb{B}}], \\ \mathbb{A} - \mathbb{B} &= [\underline{\mathbb{A}} - \overline{\mathbb{B}}, \overline{\mathbb{A}} - \underline{\mathbb{B}}], \\ \mathbb{A} \times \mathbb{B} &= \big[\min(\underline{\mathbb{A}}\underline{\mathbb{B}}, \underline{\mathbb{A}}\overline{\mathbb{B}}, \overline{\mathbb{A}}\underline{\mathbb{B}}, \overline{\mathbb{A}}\overline{\mathbb{B}}), \max(\underline{\mathbb{A}}\underline{\mathbb{B}}, \underline{\mathbb{A}}\overline{\mathbb{B}}, \overline{\mathbb{A}}\underline{\mathbb{B}}, \overline{\mathbb{A}}\overline{\mathbb{B}})\big], \\ \mathbb{A} \div \mathbb{B} &= \mathbb{A} \times [1/\overline{\mathbb{B}}, 1/\underline{\mathbb{B}}], \quad \text{if } 0 \notin \mathbb{B}. \end{aligned} \tag{4.2}$$

Note that the identities (4.2) reduce to ordinary real arithmetic when the intervals are *thin*, i.e., when $\underline{\mathbb{A}} = \overline{\mathbb{A}}$ and $\underline{\mathbb{B}} = \overline{\mathbb{B}}$. When computing with finite precision, however, directed rounding must also be taken into account, see, e.g., [20,21]. A key feature of interval arithmetic is that it is *inclusion monotonic*, i.e., if $\mathbb{A} \subseteq \mathbb{X}$, and $\mathbb{B} \subseteq \mathbb{Y}$, then

$$\mathbb{A} \star \mathbb{B} \subseteq \mathbb{X} \star \mathbb{Y}, \tag{4.3}$$

where we demand that $0 \notin \mathbb{Y}$ for division.

One of the main reasons for passing to the interval arithmetic is that this approach provides a simple way of enclosing the range of a function f, denoted by $\text{range}(f; D) := \{f(x)\colon\ x \in D\}$. Except for the most trivial cases, classical mathematics provides few tools to accurately bound the range of a function. To achieve this latter goal, we extend the real functions to *interval functions* which take and return intervals rather than real numbers. Based on (4.2) we extend rational functions to their interval versions by simply substituting all occurrences of the real variable x with the interval variable $\mathbb{X}$ (and the real arithmetic operators with their interval counterparts). This produces a rational interval function $F(\mathbb{X})$, called the *natural interval extension* of f. As long as no singularities are encountered, we have the inclusion

$$\text{range}(f; \mathbb{X}) \subseteq F(\mathbb{X}), \tag{4.4}$$

by property (4.3). In fact, this type of range enclosure can be achieved for any reasonable function. Higher-dimensional functions $f : \mathbb{R}^n \to \mathbb{R}$ can be extended to an interval function

$F:\mathbb{IR}^n \to \mathbb{IR}$ in a similar manner. The function argument is then an interval-vector $\mathbb{X} = (\mathbb{X}_1, \dots, \mathbb{X}_n)$, which we also refer to as a *box*. In particular, functions acting in the complex plane $f:\mathbb{C} \to \mathbb{C}$ can be extended, although finding good quality range enclosures of the elementary functions is much more complicated than in the real-valued setting.[3]

There exist several open source programming packages for interval analysis [3,9,23], as well as commercial products such as [25].

4.2. The main algorithm

The aim of the computational part of the proof of Theorem 3.1 is to show that (4.1) holds. To achieve this objective, the four branches of the spectrum $\Sigma_1, \dots, \Sigma_4$ from (2.14) are extended to accept entire boxes $\mathbb{B}$ of parameters as input, and to return rectangles in the complex plane containing the range of the original functions:

$$\text{range}(\Sigma_i; \mathbb{B}) \subseteq \Sigma_i(\mathbb{B}).$$

We will work with the global parameter domain

$$(\theta, \kappa, x, y) \in \left(\left[\frac{\pi}{200}, \pi\right], \left[\frac{1}{40}, \frac{9}{10}\right], \left\{\frac{1}{2}\right\}, [0, 10000]\right),$$

which corresponds to fixing $p = 2$ (again, in the light of (2.15)–(2.16) there is no loss of generality in assuming that $\theta \in [\frac{\pi}{200}, \pi]$ and $y \in [0, 10^4]$). This domain will be adaptively partitioned until (3.2) holds true on each subdomain. On each subdomain $\mathbb{B}$, we compute

$$\bar{\rho} = \bar{\rho}(\mathbb{B}) := \max\left\{\overline{|\Sigma_i(\mathbb{B})|}\colon i = 1, \dots, 4\right\},$$

which gives an upper bound on spectral radius. We also compute $\underline{R} = \underline{R}(\mathbb{B})$ via an interval extension of (3.1). Note that the function R is real-valued and does not depend on the parameter y. The main algorithm driving the program is presented in Algorithm 4.1.

Algorithm 4.1.

```
searchList += initialDomain;                // Add one box to the search list.
while ( !IsEmpty(searchList) ) {
  BOX  param = Pop(searchList);             // The current parameter box.
  real rho   = MaxReal;                     // The modulus to be computed.
  if ( !computeModulus(rho, param) || !conjectureTrue(rho, param) )
    splitAndStore(param, searchList);
  else
    verifiedList += param;                  // Just for bookkeeping.
  }
}
```

This algorithm uses some special features of the `C/C++` programming languages. On the row

[3] We thank Markus Neher and Ingo Eble for developing CoStLy—Complex interval Standard functions Library, and for their valuable assistance with interfacing it to the CXSC library [3].

```
if ( !computeModulus(rho, param) || !conjectureTrue(rho, param) )
```

the symbols `!` and `||` mean `not` and `or`, respectively. When determining whether the `if`-statement should be performed or not, the boolean function `computeModulus` is executed first. If this fails to compute the modulus ρ, it returns the value `false`, and the parameter box is partitioned and stored in `searchList`. The computation can fail due to overestimation when the parameter boxes are still quite large. *Only* if we succeed in computing the modulus is the second part of the `if`-statement executed. This part, illustrated in Algorithm 4.3, simply computes a lower bound for the spectral radius R (based (1.4)), and checks whether or not $\overline{\rho} \leqslant \underline{R} + \varepsilon$, for some given $\varepsilon > 0$.

The boolean function `computeModulus` (listed in Algorithm 4.2) attempts to compute an upper bound ρ of the spectral radius, using the parametric representations of the spectrum (2.14).

Algorithm 4.2.

```
bool computeModulus(real &rho, BOX param)
{
  CRECT A, B, C, D, E;
  computeCmplABCDE(A,B,C,D,E,param);
  interval L  = param[2];
  CRECT Qpos  = sqr(B) + sqr(L*C) - sqr(L*E + A*B);
  CRECT Qneg  = sqr(B) + sqr(L*C) - sqr(L*E - A*B);

  CRECT nominator = sqrt(Qpos) + A*C;
  rho = Sup(abs(nominator/D));              // Branch #1.
  nominator = sqrt(Qpos) - A*C;
  rho = max(rho, Sup(abs(nominator/D)));    // Branch #2.
  nominator = sqrt(Qneg) + A*C;
  rho = max(rho, Sup(abs(nominator/D)));    // Branch #3.
  nominator = sqrt(Qneg) - A*C;
  rho = max(rho, Sup(abs(nominator/D)));    // Branch #4.
  return true;
}
```

When carrying out the computations, the actual implementation of Algorithm 4.2 is adapted to minimize the number of arithmetic operations. Finally, the simple module `conjectureTrue` checks whether or not the computed bounds are good enough to (locally) verify (4.1).

Algorithm 4.3.

```
bool conjectureTrue(real rho, BOX param)
{
  real R = Inf(spectralRadius(param));      // Compute R via (3.1).
  if ( rho <= R + eps )
    return true;                            // The conjecture is true.
  else
    return false;                           // The conjecture is unproven.
}
```

4.3. Computational results

The algorithms described above were coded into a C++ program using the CXSC interval package [3]. The code was executed through five processes, running in parallel on a dual 1.5 GHz

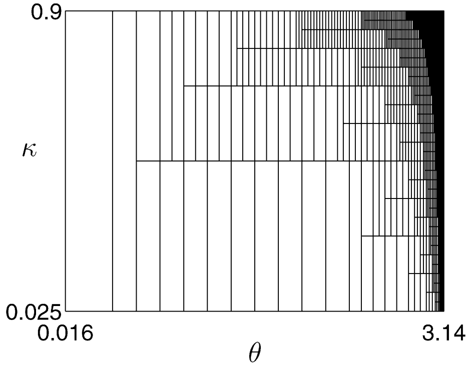

Fig. 1. The final partition of the (θ, κ)-plane with $x = \frac{1}{2}$ and $\mathbb{Y} = [2000, 10\,000]$.

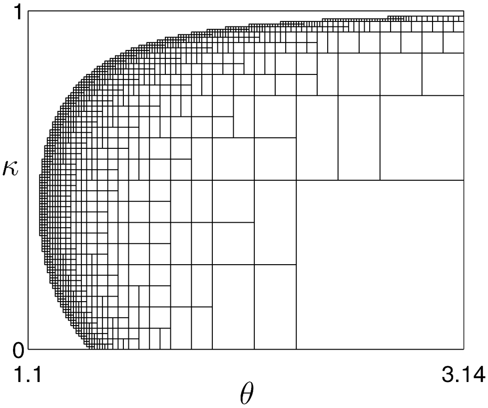

Fig. 2. A region satisfying $R(\theta, 1/2, \kappa) + 10^{-2} < 1$.

AMD Athlon MP 1800+, and a dual 3.2 GHz Intel Xeon processor, both having 3072 Mb RAM. Proving then the inequality (4.1) for $(\theta, \kappa, x, y) \in ([\frac{\pi}{200}, \pi], [\frac{1}{40}, \frac{9}{10}], \{\frac{1}{2}\}, [0, 10\,000])$, which corresponds to taking $\varepsilon = 0.01$ in the Algorithm 4.3, took 16 hours.

The computations were most intense for small values of y. This is in agreement with the conjecture that the spectral radius is attained for $y = 0$, and then coincides with the corresponding value of R. As a consequence, only small y-slices (of width 1×10^{-3}) could be handled for small y, whereas the final y-slice could be taken as $\mathbb{Y} = [2000, 10\,000]$! Regarding the parameters θ and κ, the conjecture proved most challenging for θ near π, and κ large, see Fig. 1.

Next, we computed the region in the (θ, κ)-space for which the inequality $R(\theta, 1/2, \kappa) + 10^{-2} < 1$ holds. This was done by finding all parameter boxes for which $\overline{R} + \varepsilon < 1$. Setting the stopping tolerance (i.e., the smallest acceptable side length of a parameter box) to 10^{-2} produced the set illustrated in Fig. 2. See Theorems 5.1 and 5.5 for related results.

5. The connection with the spectral radius conjecture

Recall that Ω is an infinite sector in $\mathbb{R}^2$ with aperture $\theta \in (0, 2\pi)$. In this section we show that the conjectured value for $\rho(K; L^p(\partial\Omega))$ is < 1 for all $\theta \in (0, 2\pi)$, $\mu > 0$ and $\lambda + \mu > 0$, and

$p \in [2, \infty)$, and we identify a class of curvilinear polygons in $\mathbb{R}^2$ for which the spectral radius conjecture holds. We have

Theorem 5.1. *For any $\alpha \in [0, \pi)$, $x \in (0, \frac{1}{2}]$ and $\kappa \in (0, 1)$ the following holds*

$$R(\alpha, x, \kappa) < 1, \tag{5.1}$$

where $R(\alpha, x, \kappa)$ is as in (3.1).

We start by presenting a series of technical lemmas useful in the proof of Theorem 5.1.

Lemma 5.2. *The following two inequalities hold*:

$$\sin(\gamma x) > x \sin(\gamma), \quad \forall x \in (0, 1),\ \gamma \in (0, \pi), \tag{5.2}$$

and

$$\sin\bigl((\pi + \gamma)x\bigr) > x \sin(\gamma), \quad \forall x \in \left(0, \frac{1}{2}\right),\ \gamma \in (0, \pi). \tag{5.3}$$

Proof. Fix $x \in (0, 1)$ and consider $h : (0, \pi) \to \mathbb{R}$ given by $h(\gamma) := \sin(\gamma x) - x \sin(\gamma)$. Then $h'(\gamma) = x[\cos(\gamma x) - \cos(\gamma)] > 0$, where the inequality follows from the fact that cosine is monotonically decreasing on the interval $(0, \pi)$ and $0 < \gamma x < \gamma < \pi$. Then, $h(\gamma) > h(0) = 0$ and the proof of (5.2) is completed.

Next, our goal is to prove (5.3). To this end, fix $x \in (0, \frac{1}{2})$ and consider the function $g : (0, \pi) \to \mathbb{R}$ given by $g(\gamma) := \sin((\pi + \gamma)x) - x \sin(\gamma)$. Differentiating with respect to the variable γ we obtain $g'(\gamma) = x[\cos((\pi + \gamma)x) - \cos(\gamma)]$. Now, using again the monotonicity of the cosine function on the interval $(0, \pi)$ and the hypothesis, a simple analysis reveals that $f'(\gamma) < 0$ for $\gamma \in (0, \gamma_0)$, $f'(\gamma) > 0$ for $\gamma \in (\gamma_0, \pi)$, and $f'(\gamma_0) = 0$, where

$$\gamma_0 := \frac{\pi x}{1 - x} \in (0, \pi). \tag{5.4}$$

Therefore, for any $\gamma \in [0, \pi)$ we have that $f(\gamma) \geqslant f(\gamma_0) = (1 - x)\sin(\gamma_0) > 0$. This gives (5.3), as desired. □

Lemma 5.3. *For any $\alpha \in [0, \pi)$, $x \in (0, \frac{1}{2}]$ and $\kappa \in (0, 1)$ we have*

$$\sin(\pi x) - (1 - \kappa)x \sin(\alpha)\cos(\alpha x) > 0. \tag{5.5}$$

Proof. Notice that $x \sin(\alpha)\cos(\alpha x) \geqslant 0$ whenever $\alpha \in [0, \pi)$ and $x \in (0, \frac{1}{2}]$ as all the trigonometric functions involved yield positive values. Therefore

$$\sin(\pi x) - (1 - \kappa)x \sin(\alpha)\cos(\alpha x) \geqslant \sin(\pi x) - x \sin(\alpha)\cos(\alpha x). \tag{5.6}$$

Now, using the identities $\sin(\pi x) = \sin(\alpha x)\cos((\pi - \alpha)x) + \cos(\alpha x)\sin((\pi - \alpha)x)$ together with $\sin(\alpha) = \sin(\pi - \alpha)$, the right-hand side of (5.6) can be rewritten as

$$\sin(\alpha x)\cos\bigl((\pi - \alpha)x\bigr) + \bigl[\sin\bigl((\pi - \alpha)x\bigr) - x \sin(\pi - \alpha)\bigr]\cos(\alpha x). \tag{5.7}$$

Invoking next (5.2) for $\gamma = \pi - \alpha \in (0, \pi]$ we conclude that $\sin((\pi - \alpha)x) - x\sin(\pi - \alpha) > 0$ for x and α as in the hypothesis. This, together with $\sin(\alpha x) \geqslant 0$, $\cos((\pi - \alpha)x) \geqslant 0$, and $\cos(\alpha x) > 0$ for $x \in (0, \frac{1}{2}]$ and $\alpha \in [0, \pi)$, allow us to conclude that the expression in (5.7) is strictly positive. This gives (5.5). □

Lemma 5.4. *For any $x \in (0, \frac{1}{2}]$ and $\alpha \in [0, \pi)$ the following inequalities hold*:

$$\cos^2(\alpha x) - \cos^2(\pi x) - x^2 \sin^2(\alpha) - 2x \sin(\alpha)\sin(\alpha x)\cos(\pi x) > 0, \tag{5.8}$$

and

$$\cos^2(\alpha x) - \cos^2(\pi x) + x^2 \sin^2(\alpha) - 2x \sin(\alpha)\cos(\alpha x)\sin(\pi x) > 0. \tag{5.9}$$

Proof. The case $\alpha = 0$ follows immediately. For the remaining of the proof we consider the case $\alpha \in (0, \pi)$. Set

$$g(y) := ay^2 + by + c, \quad \text{where} \begin{cases} a := -\sin^2(\alpha), \\ b := -2\sin(\alpha)\sin(\alpha x)\cos(\pi x), \\ c := \cos^2(\alpha x) - \cos^2(\pi x). \end{cases} \tag{5.10}$$

Straightforward algebraic manipulations show that the discriminant Δ of the quadratic expression in (5.10) and its two roots y_1 and y_2 are given by

$$\Delta = 4\sin^2(\alpha)\cos^2(\alpha x)\sin^2(\pi x), \qquad y_1 = -\frac{\sin(\pi + \alpha x)}{\sin(\alpha)}, \qquad y_2 = \frac{\sin((\pi - \alpha)x)}{\sin(\alpha)}. \tag{5.11}$$

Next, for $x \in (0, \frac{1}{2}]$ and $\alpha \in [0, \pi)$ we have $y_1 < 0$ and $y_2 \geqslant 0$ and $y_1 < x < y_2$, where the fact that $x < y_2$ follows from (5.2). Consequently, since $a < 0$, we obtain that $g(x) > 0$ and this finishes the proof of (5.8) in Lemma 5.4.

Turning attention to (5.9), we consider the quadratic function

$$h(y) := \tilde{a}y^2 + \tilde{b}y + \tilde{c}, \quad \text{where} \begin{cases} \tilde{a} := \sin^2(\alpha), \\ \tilde{b} := -2\sin(\alpha)\cos(\alpha x)\sin(\pi x), \\ \tilde{c} := \cos^2(\alpha x) - \cos^2(\pi x). \end{cases} \tag{5.12}$$

Denoting by $\tilde{\Delta}$ the discriminant associated with (5.12) and by $\tilde{y}_1$ and $\tilde{y}_2$ the roots of the polynomial h, straightforward computations give

$$\tilde{\Delta} = 4\sin^2(\alpha)\sin^2(\alpha x)\cos^2(\pi x), \qquad \tilde{y}_1 = \frac{\sin((\pi + \alpha)x)}{\sin(\alpha)}, \qquad \tilde{y}_2 = \frac{\sin((\pi - \alpha)x)}{\sin(\alpha)}. \tag{5.13}$$

Appealing to (5.2)–(5.3) and using that $\sin(\alpha) > 0$ for $\alpha \in (0, \pi)$ we conclude that $\tilde{y}_i > x$ for $i = 1, 2$. Since $\tilde{a} > 0$, this implies $h(x) > 0$ and the proof of (5.9) is now finished. □

After this preamble, we are ready to present the

Proof of Theorem 5.1. Recall that $R(\alpha, x, \kappa) = \{\sqrt{E(\alpha, x, \kappa)} + (1-\kappa)x\sin(\alpha)\cos(\alpha x)\}\frac{1}{\sin(\pi x)}$, where $E(\alpha, x, \kappa)$ is as in (3.5). Then, it is immediate that (5.1) can be reformulated in the equivalent form

$$\sqrt{E(\alpha, x, \kappa)} < \sin(\pi x) - (1-\kappa)x\sin(\alpha)\cos(\alpha x), \tag{5.14}$$

for all α, x and κ as in the hypothesis. To prove (5.14), fix $\alpha \in [0, \pi)$, $x \in (0, \frac{1}{2}]$ and $\kappa \in (0, 1)$, and notice that, by invoking Lemma 5.3 matters are reduced to proving that

$$0 < \big(\sin(\pi x) - (1-\kappa)x\sin(\alpha)\cos(\alpha x)\big)^2 - E(\alpha, x, \kappa) =: (1-\kappa)g(\alpha, x, \kappa). \tag{5.15}$$

Straightforward algebraic manipulations based on (3.5) give that

$$\begin{aligned} g(\alpha, x, \kappa) = {} & (1+\kappa)\big[\cos^2(\alpha x) - \cos^2(\pi x)\big] + (1-\kappa)x^2\sin^2(\alpha) \\ & - 2x\sin(\alpha)\big[\kappa\sin(\alpha x)\cos(\pi x) + \cos(\alpha x)\sin(\pi x)\big]. \end{aligned} \tag{5.16}$$

Differentiating with respect to κ in the expression above, we obtain that

$$\frac{\partial g}{\partial \kappa}(\alpha, x, \kappa) \quad \text{equals the left-hand side of (5.8).} \tag{5.17}$$

Now, using Lemma 5.4, this further implies that $g(\alpha, x, \kappa) \geqslant g(\alpha, x, 0) > 0$. The last inequality follows from the fact that $g(\alpha, x, 0)$ equals the expression in the left-hand side of (5.9), which by Lemma 5.4, is strictly positive. This gives (5.15) and the proof of the Theorem 5.1 is completed. □

Next, let Ψ denote the space of vector valued functions ψ on $\mathbb{R}^2$ satisfying the equations $\partial_i\psi^j + \partial_j\psi^i = 0$, $i, j = 1, 2$, restricted to $\partial\Omega$. Then, the rigorous computations carried out for producing Fig. 2 have the following consequence.

Theorem 5.5. *Let Ω be a curvilinear polygon in $\mathbb{R}^2$ with angles in the interval $[\frac{23\pi}{50}, 2\pi - \frac{23\pi}{50}]$ and assume that the Lamé moduli μ, λ satisfy $\kappa := \frac{\mu}{2\mu+\lambda} \in [\frac{1}{40}, \frac{9}{10}]$. Then*

$$\rho\big(K; L^2(\partial\Omega)/\Psi\big) < 1. \tag{5.18}$$

Moreover,

$$\rho\big(K; L^p(\partial\Omega)/\Psi\big) < 1 \quad \text{for all } 2 \leqslant p < \infty. \tag{5.19}$$

Proof. In the light of Theorem 6.1 in [19] and (2.15) matters reduce to showing (5.18) when Ω is an infinite sector of aperture $\theta \in [\frac{23\pi}{50}, \pi]$. However, using Theorem 3.1 in this scenario (for θ and κ as in the hypothesis) gives

$$\rho\big(K; L^2(\partial\Omega)\big) < R(\theta, 1/2, \kappa) + 10^{-2} < 1. \tag{5.20}$$

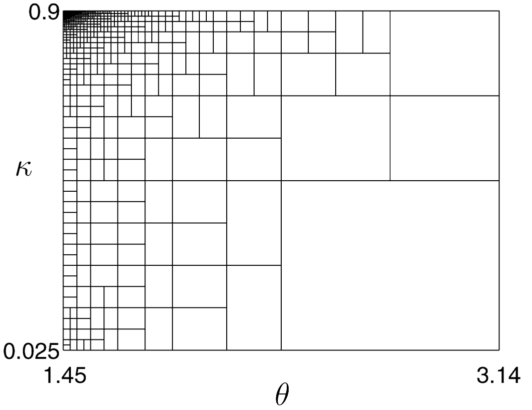

Fig. 3. The final subdivision for verifying $R(\theta, 1/2, \kappa) + 10^{-2} < 1$.

Figure 3 illustrates how the region $[\frac{23\pi}{50}, \pi] \times [\frac{1}{40}, \frac{9}{10}]$ was subdivided when rigorously checking using the computer (see the discussion at the end of Section 4) that the last inequality in (5.20) holds.

As for (5.19), this immediately follows from (5.18) and Theorem 5.6 in [19]. □

Finally, let us point out that the condition $\kappa := \frac{\mu}{2\mu+\lambda} \in [\frac{1}{40}, \frac{9}{10}]$ is satisfied for the following common elastic materials (see [2, p. 129]; here the Lamé moduli λ and μ are given in 10^5 kg/cm^2) (see Table 1).

Table 1

Elastic material	λ	μ	κ	Elastic material	λ	μ	κ
Iron	9.9	7.8	0.3059	Copper	8.7	4.1	0.2426
Bronze	6.2	3.8	0.2754	Aluminum	5.6	2.6	0.2407
Nickel	1.3	0.85	0.2833	Rubber	0.40	0.012	0.0283
Glass	2.2	2.2	1/3	Lead	4.6	0.63	0.0467
Steel	10	8.2	0.3106				

References

[1] G. Alefeld, J. Herzberger, Introduction to Interval Computations, Academic Press, New York, 1983.

[2] P.G. Ciarlet, Mathematical Elasticity, vol. 1: Three-Dimensional Elasticity, Stud. Math. Appl., vol. 20, North-Holland, Amsterdam, 1988.

[3] CXSC—C++ eXtension for Scientific Computation, version 2.0, available from http://www.math.uni-wuppertal.de/org/WRST/xsc/cxsc.html.

[4] B. Dahlberg, C. Kenig, G. Verchota, Boundary value problems for the system of elastostatics on Lipschitz domains, Duke Math. J. 57 (1988) 795–818.

[5] J. Elschner, The double layer potential operator over polyhedral domains, I: Solvability in weighted Sobolev spaces, Appl. Anal. 45 (1992) 117–134.

[6] L. Escauriaza, E.B. Fabes, G. Verchota, On a regularity theorem for weak solutions to transmission problems with internal Lipschitz boundaries, Proc. Amer. Math. Soc. 115 (4) (1992) 1069–1076.

[7] E.B. Fabes, M. Jodeit, J.E. Lewis, On the spectra of a Hardy kernel, J. Funct. Anal. 21 (1976) 187–194.

[8] N.V. Grachev, V.G. Maz'ya, The Fredholm radius of integral operators of potential theory, J. Soviet Math. 64 (6) (1993) 1297–1313 (in Russian).

[9] INTLAB—INTerval LABoratory, version 4.1.2, available from http://www.ti3.tu-harburg.de/~rump/intlab/.
[10] C.E. Kenig, Harmonic Analysis Techniques for Second Order Elliptic Boundary Value Problems, CBMS Reg. Conf. Ser. Math., vol. 83, Amer. Math. Soc., Providence, RI, 1994.
[11] V. Kozlov, V.G. Maz'ya, J. Rossmann, Spectral properties of operator pencils generated by elliptic boundary value problems for the Lamé system, Rostock. Math. Kolloq. 51 (1997) 5–24.
[12] G.I. Kresin, V.G. Maz'ya, The norm and the essential norm of the double layer elastic and hydrodynamic potentials in the space of continuous functions, Math. Methods Appl. Sci. 18 (14) (1995) 1095–1131.
[13] U.W. Kulisch, W.L. Miranker, Computer Arithmetic in Theory and Practice, Academic Press, 1981.
[14] V.D. Kupradze, Potential Methods in the Theory of Elasticity, Israel Program for Scientific Translations, Jerusalem, 1965.
[15] J.E. Lewis, A symbolic calculus for layer potentials on $\mathcal{C}^1$ curves and $\mathcal{C}^1$ curvilinear polygons, Proc. Amer. Math. Soc. 112 (2) (1991) 419–427.
[16] J.E. Lewis, Layer potentials for elastostatics and hydrostatics in curvilinear domains, Trans. Amer. Math. Soc. 320 (1) (1990) 53–76.
[17] I. Mitrea, Spectral radius properties for layer potentials associated with the elastostatics and hydrostatics equations in nonsmooth domains, J. Fourier Anal. Appl. 5 (3) (1999) 389–412.
[18] I. Mitrea, On the spectra of elastostatic and hydrostatic layer potentials on curvilinear polygons, J. Fourier Anal. Appl. 8 (2002) 1–66.
[19] I. Mitrea, On the traction problem for the Lamé system on curvilinear polygons, J. Integral Equations Appl. 16 (2) (2004) 175–219.
[20] R.E. Moore, Interval Analysis, Prentice Hall, Englewood Cliffs, NJ, 1966.
[21] R.E. Moore, Methods and Applications of Interval Analysis, SIAM Studies in Applied Mathematics, Philadelphia, 1979.
[22] A. Neumaier, Interval Methods for Systems of Equations, Encyclopedia Math. Appl., vol. 37, Cambridge Univ. Press, Cambridge, 1990.
[23] PROFIL/BIAS—Programmer's Runtime Optimized Fast Interval Library/Basic Interval Arithmetic Subroutines, available from http://www.ti3.tu-harburg.de/Software/PROFILEnglisch.html.
[24] V.Y. Shelepov, On the index and spectrum of integral operators of potential type along Radon curves, Math. USSR Sb. 70 (1) (1991) 175–203.
[25] Forte Developer 7: C++ Interval Arithmetic Programming Reference, available from http://docs.sun.com/app/docs/doc/816-2465.
[26] W. Tucker, The Lorenz attractor exists, C. R. Acad. Sci. Paris Sér. I Math. 328 (12) (1999) 1197–1202.
[27] W. Tucker, A rigorous ODE solver and Smale's 14th problem, Found. Comput. Math. 2 (1) (2002) 53–117.
[28] G.C. Verchota, Layer potentials and regularity for the Dirichlet problem for Laplace's equation in Lipschitz domains, J. Funct. Anal. 69 (1984) 572–611.